Optical pulse coding in hybrid distributed sensing based on Raman and Brillouin scattering employing Fabry–Perot lasers

Gabriele Bolognini* and Marcelo A. Soto

Scuola Superiore Sant'Anna, via G. Moruzzi 1, 56124 Pisa, Italy
**gabriele.bolognini@sssup.it*

Abstract: We demonstrate simultaneous strain and temperature sensing based on hybrid Raman and Brillouin scattering with enhanced performance thanks to the combined use of standard Fabry–Perot lasers in conjunction with optical pulse coding techniques. The combination of both techniques allows for an improvement of ~8.7 dB in temperature resolution and ~3 dB in strain resolution, with respect to standard distributed feedback lasers, as confirmed by experiments, resulting in a final temperature / strain resolution of ~0.27K / ~30με over 25-km sensing fiber range, avoiding the use of optical amplification and wavelength averaging techniques.

OCIS codes: (060.2370) Fiber optics sensors; (290.5830) Scattering, Brillouin; (290.5860) Scattering, Raman.

References and links

1. "Great potential," Nat. Photonics **2**(3), 143–158 (2008).
2. T. R. Parker, M. Farhadiroushan, V. A. Handerek, and A. J. Roger, "A fully distributed simultaneous strain and temperature sensor using spontaneous Brillouin backscatter," IEEE Photon. Technol. Lett. **9**(7), 979–981 (1997).
3. C. C. Lee, P. W. Chiang, and S. Chi, "Utilization of a Dispersion-Shifted Fiber for Simultaneous Measurement of Distributed Strain and Temperature Through Brillouin Frequency Shift," IEEE Photon. Technol. Lett. **13**(10), 1094–1096 (2001).
4. M. N. Alahbabi, Y. T. Cho, and T. P. Newson, "Simultaneous temperature and strain measurement with combined spontaneous Raman and Brillouin scattering," Opt. Lett. **30**(11), 1276–1278 (2005).
5. W. Zou, Z. He, and K. Hotate, "Investigation of strain- and temperature-dependences of Brillouin frequency shifts in GeO_2-doped optical fibers," J. Lightwave Technol. **26**(13), 1854–1861 (2008).
6. G. Bolognini, M. A. Soto, and F. Di Pasquale, "Fiber-optic distributed sensor based on hybrid Raman and Brillouin scattering employing multi-wavelength Fabry-Pérot lasers," IEEE Photon. Technol. Lett. **21**(20), 1523–1525 (2009).
7. G. Bolognini, J. Park, M. A. Soto, N. Park, and F. Di Pasquale, "Analysis of distributed temperature sensing based on Raman scattering using OTDR coding and discrete Raman amplification," Meas. Sci. Technol. **18**(10), 3211–3218 (2007).
8. K. De Souza, "Significance of coherent Rayleigh noise in fibre-optic distributed temperature sensing based on spontaneous Brillouin scattering," Meas. Sci. Technol. **17**(5), 1065–1069 (2006).
9. M. A. Soto, G. Bolognini, and F. Di Pasquale, "Analysis of optical pulse coding in spontaneous Brillouin-based distributed temperature sensors," Opt. Express **16**(23), 19097–19111 (2008).

1. Introduction

Optical-fiber distributed sensors provide a photonic-based enabling technology which encompasses a growing variety of applications, from structural-health monitoring, to leakage and deformation detection in pipelines, boreholes and power cables, from landslide warning to fire detection in reservoirs and tunnels [1]. A great part of distributed optical fiber sensors enables strain or temperature measurements. Those sensors allowing for simultaneous strain *and* temperature measurements are mostly based either on Brillouin scattering effect [2,3] or on combined Raman–Brillouin scattering effects [4], typically in conjunction with interrogating techniques based on optical time domain reflectometry (OTDR).

For the hybrid sensing techniques that are based on combined Raman–Brillouin scattering, spontaneous Raman scattering (SpRS), which does not depend on strain, is exploited to directly infer the fiber temperature profile. The strain sensitivity is provided by the Brillouin

#124144 - $15.00 USD Received 11 Feb 2010; revised 11 Mar 2010; accepted 12 Mar 2010; published 7 Apr 2010

scattering, through its dependence on the fiber sound velocity [5]; unfortunately, the most strain-sensitive parameter, i.e. the Brillouin frequency shift (BFS), also exhibits a notable cross-sensitivity to fiber temperature. Hence, in order to provide temperature-independent strain estimation, the temperature profile obtained from SpRS is used in BFS calibration.

In combined Raman–Brillouin sensors, the difference in cross-sections for Brillouin and Raman scattering leads to significantly different backscattered power levels (actually the Brillouin-scattering cross-section is typically about one order of magnitude larger than the Raman cross-section), thus causing significant impairments in temperature-strain resolution. In fact, the limiting factor in combined Raman–Brillouin sensors has been identified to be due to the noise in low-power SpRS based temperature measurements [4]. Since it is not simple or cost-effective to use two different light sources for SpRS and Brillouin scattering, then one straightforward solution is given by an increase in input light power. However, the onset of optical nonlinear effects creates a constraint in the maximum usable input power level, limiting this below a given threshold value. In order to overcome this limitation, an effective sensing scheme based on the use of multiple longitudinal modes lasers has been recently reported [6], allowing for higher usable pump peak power values as well as a reduced level in coherent Rayleigh noise (CRN) [8].

In this paper, we propose the use of optical pulse coding in combination with standard high-power Fabry–Perot (FP) lasers to achieve high-resolution strain and temperature measurements in combined Raman-Brillouin sensing. Actually, considering that the typical peak power of *each* FP mode is far below the nonlinear threshold level, it is possible to use pulse coding techniques [9] to improve the signal-to-noise ratio (SNR) in both Raman and Brillouin traces, showing a particular benefit for low-power noisy Raman measurements and finally leading to a notable performance improvement in combined sensing.

2. Theory

In distributed hybrid Raman–Brillouin sensors, both the anti-Stokes SpRS power and the BFS are simultaneously measured [4]. While the anti-Stokes SpRS is sensitive to temperature variations only, the BFS allows for both temperature and strain measurements. Since, when measuring the BFS it is inherently impossible to separate temperature from strain changes, the strain-independent temperature measurements provided by Raman measurements constitute a very attractive solution to perform simultaneous strain-temperature sensing using a single fiber. In such a scheme, the fiber temperature (T) is obtained by anti-Stokes SpRS power traces. However, to take into account fiber loss, the ratio of Rayleigh-backscattered power (P_{Ray}) over anti-Stokes Raman power (P_{AS}) is typically used, providing the following equation:

$$\frac{P_{Ray}(z)}{P_{AS}(z)} \propto \frac{P_{Ray}(z)}{P_{AS}(T,z)} \exp\left\{-\int_0^z \left[\alpha_{Ray}(z) - \alpha_{AS}(z)\right] \cdot d\varsigma\right\} \qquad (1)$$

where $R_{Ray}(z)$ is the Rayleigh backscattering coefficient, $R_{AS}(T,z)$ is the temperature-dependent Raman backscattering coefficient (from [7]), α_{Ray} and α_{AS} are the loss coefficients at Rayleigh and AS-Raman light wavelengths respectively. Equation (1) allows one to infer the fiber temperature with respect to one known reference value at a given point, provided that the attenuation coefficients (α_{Ray}, α_{AS}) for the optical fiber are known [7]. For narrowband sources, the Rayleigh backscattered light from a given fiber location is phase-correlated with the backscattered light from other fiber locations, giving rise to noisy interference patterns (known as CRN [8]) at the receiver-side, affecting the Rayleigh trace. This effect cannot be reduced through trace averaging, thus requiring techniques to increase the source bandwidth, or, equivalently, to reduce the source coherence length. Once temperature (ΔT) and BFS ($\Delta \nu_B$) variations along the fiber are obtained, this information can be used in conjunction to strain and temperature coefficients for BFS ($C_{\nu B\varepsilon}$ = 0.048 MHz/με and $C_{\nu BT}$ = 1.10 MHz/°C [2]) to obtain the distributed strain profile ($\Delta\varepsilon$) according to:

#124144 - $15.00 USD Received 11 Feb 2010; revised 11 Mar 2010; accepted 12 Mar 2010; published 7 Apr 2010

$$\Delta\varepsilon(z) = \frac{\Delta\nu_B(z) - C_{\nu_B T} \cdot \Delta T(z)}{C_{\nu_B \varepsilon}} \tag{2}$$

In order to improve the performance of distributed hybrid sensors, the use of multi-wavelength sources, such as FP lasers, has been recently proposed [6]. Actually, the peak power launched into the fiber when using FP laser is distributed among several longitudinal modes along the spectrum, overcoming the main limiting nonlinearities, such as stimulated Brillouin scattering (SBS) and modulation instability (MI), which become particularly relevant when narrowband sources are used. The limiting factor in hybrid sensing is actually given by the noise affecting the low-power anti-Stokes Raman measurements [4]; however, the proposed broadband source allows for the use of high peak power levels, resulting in higher SNR and leading then to a better temperature and strain resolution.

On the other hand, the use of optical pulse coding has been recently proposed for distributed sensing based on spontaneous Brillouin scattering [9], offering an effective technique to improve the SNR of the measurements, and hence to enhance the sensing performance. However, coding techniques unfortunately also reduce the SBS threshold, and, for instance, when using 127-bit Simplex coding with single longitudinal mode lasers (e.g. DFB lasers) and ~350 ns pulses, the SBS threshold power is decreased from ~30 dBm (with single pulses) down to ~10 dBm. Considering that the SBS threshold only limits the peak power per FP mode, then the use of pulse coding with no induced distortion is possible even with high-power FP lasers, since in typical conditions the power of *each* FP mode remains below the SBS threshold. However, even though the use of FP lasers in single-pulse schemes enhances the sensing performance, the noise in SpRS traces is still a limiting factor [9]. Note that, while the temperature resolution depends only on the SNR of the Raman measurements, the strain resolution depends on both BFS and temperature resolution. Thus, the use of optical pulse coding in principle allows for higher resolution on Raman power and BFS measurements, leading to a much better sensing performance. In this paper, then, we experimentally show that the combination of both FP lasers and pulse coding allows for a significant SNR enhancement in both anti-Stokes Raman power and BFS measurements.

3. Experimental setup

To evaluate the distributed Brillouin–Raman sensor performance provided by the combination of FP lasers with optical pulse coding techniques, the experimental setup shown in Fig. 1 has been implemented. Two optical sources, a FP laser and a DFB laser, have been used to compare the performance of the proposed technique with respect to the conventional hybrid sensor based on a single longitudinal mode laser. Since the FP laser allows for more optical power at the fiber input than the DFB laser, an Erbium-doped fiber amplifier (EDFA) has been used to amplify the DFB laser allowing for a better comparison under the same experimental conditions. The peak pulse power at the fiber input has been hence set to 15 dBm for both sources, making the use of coding impossible when employing the DFB laser, due to onset of the detrimental nonlinear effects (most notably SBS) near fiber input [9].

#124144 - $15.00 USD Received 11 Feb 2010; revised 11 Mar 2010; accepted 12 Mar 2010; published 7 Apr 2010

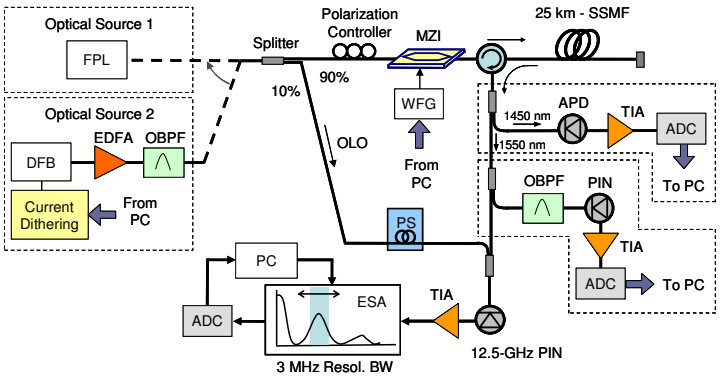

Fig. 1. Experimental set-up.

Note that when using the DFB laser, additional techniques are required to reduce CRN in the Rayleigh measurement, thus current dithering and wavelength averaging need to be also implemented. Conversely, the broadband characteristics of the FP laser allow us to inherently reduce CRN, not requiring the additional above-mentioned techniques used with single mode lasers [8]. In our experiment we have employed a high-power FP laser with ~30 longitudinal modes, inherently allowing for more than 7.3 dB measured CRN reduction in Rayleigh trace with respect to DFB lasers. Moreover, the linewidth of each FP laser mode (1-2 MHz within 100-μs scale) provides a further reduction in CRN with respect to narrowband used DFB laser (~few hundred kHz linewidth). Finally, during the averaged-trace acquisition over a timescale higher than millisecond-order, the wavelength drift of FP laser modes (induced e.g. by FP laser temperature variations) generates an inherent wavelength-averaging effect over a fraction of nanometer, which greatly suppresses CRN effects. The CW-light of the source is then split into two branches, so that 10% of it is used as optical local oscillator (OLO) at the receiver side, while the 90% of the light is modulated by a Mach-Zehnder interferometer (MZI, extinction ratio > 40dB) with 350 ns pulses from a waveform generator (WFG), allowing for 35 m spatial resolution. The use of a high extinction ratio MZI is necessary in order to avoid noise contributions due to small leaking CW light components. Since the peak power per laser mode at fiber input is ~0 dBm, which falls well below the coded-pulse SBS threshold (~10 dBm), 127-bit Simplex coding can be effectively used for further performance enhancement when using the high-power FP laser, not inducing detrimental nonlinearities. This is not possible with DFB lasers, whose total power must be limited below ~10 dBm.

The sensing fiber is given by a 25-km standard single-mode fiber (SSMF), and the receiver-side is composed of three different stages. The first two stages are direct-detection receivers for anti-Stokes Raman and Rayleigh measurements respectively, making use of an optical band-pass filter (OBPF, > 60 dB band rejection), a 10-MHz PIN photodiode for the Rayleigh traces and a 10-MHz avalanche photodiode (APD) for the Raman traces, trans-impedance amplifiers (TIA) and analog-to-digital converters (ADC). On the other hand, the third stage consists in a self-heterodyne optical detection scheme followed by an electrical coherent receiver for BFS measurements. Note that beatings with higher frequencies arising from the multi-wavelength OLO are filtered out by the receiver bandwidth (12.5 GHz), so that they do not represent an additional source of noise. To reduce polarization-induced fluctuations in the optical heterodyne process, a polarization scrambler (PS) is used to depolarize the OLO. The electrical coherent detection is performed by an optical spectrum analyzer (OSA) operating in zero-span mode, with a maximum resolution bandwidth of 3 MHz, which actually limits the spatial resolution to ~35 m, however this is not a limitation to the proposed technique.

#124144 - $15.00 USD Received 11 Feb 2010; revised 11 Mar 2010; accepted 12 Mar 2010; published 7 Apr 2010

4. Results

To demonstrate the feasibility of using optical pulse coding techniques with high-power FP lasers in distributed hybrid Raman–Brillouin sensors, we have employed in our experiment a FP laser with ~30 high-power longitudinal modes. The spectrum of the used laser at the fiber input is shown in Fig. 2a. We can clearly observe that the maximum peak power of the strongest longitudinal modes is ~0 dBm, resulting well below the SBS threshold limit of ~10 dBm for DFB lasers with 127-bit Simplex coding.

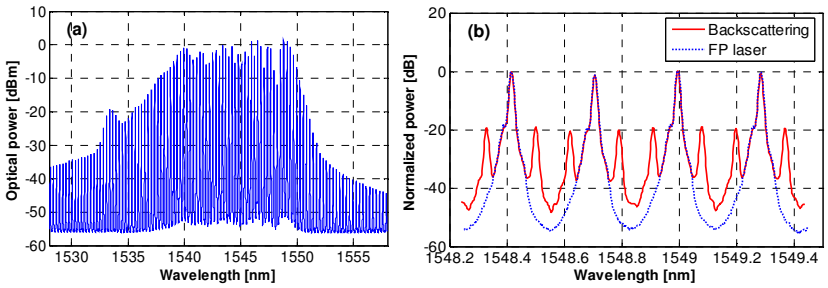

Fig. 2. (a) Full spectrum of the used FP laser and (b) detail of backscattered light spectrum.

Considering the large number of FP modes, in principle we can use up to ~25 dBm total power at the fiber input without incurring in SBS. However, the maximum power allowed at the MZI input, in our experiment, limits the usable peak power at the fiber input to a maximum of 15 dBm, resulting in the spectrum shown in Fig. 2a. This power level in narrowband sources is higher than nonlinear threshold level, thus allowing us to demonstrate the feasibility of using FP lasers with pulse coding to improve hybrid sensor performance. The normalized-power spectrum of four FP laser modes and the corresponding backscattered light are compared in Fig. 2b. We can clearly distinguish the spontaneous Brillouin scattering generated from every FP mode when using coding (exhibiting similar power levels of Stokes and anti-Stokes components around each FP mode). The beating process between the multi-wavelength OLO (obtained directly from the FP laser) and Brillouin components generates an electrical signal which corresponds to the Brillouin spectrum as shown in Fig. 3 (obtained with 150k averages).

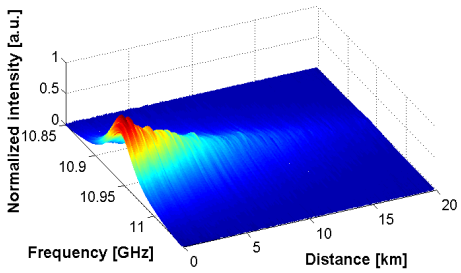

Fig. 3. Brillouin spectrum as a function of fiber distance, using FP laser with 127-bit Simplex coding.

Figure 3 shows the Brillouin spectrum along the sensing fiber when using Simplex coding, representing the contribution of all Stokes and anti-Stokes light components generated by all FP modes. We can note that no distortion of the spectrum is observed, since the power per mode keeps limited below the SBS threshold, even though the total laser peak power is higher than this value. The spectrum is then properly fitted by a Lorentzian curve in order to obtain the BFS evolution along the fiber. Actually, Fig. 4a reports the BFS obtained with both the FP laser (with both single pulses and coding) and the DFB laser (with single pulses only since coding cannot be applied), where a small difference in the BFS can be observed, mainly due to the different wavelength of the used DFB and FP lasers. By calculating the standard

#124144 - $15.00 USD Received 11 Feb 2010; revised 11 Mar 2010; accepted 12 Mar 2010; published 7 Apr 2010

deviation of the BFS along the fiber, the resolution of the measurements can be estimated, as shown in Fig. 4b. We can note in Fig. 4b that the FP laser offers a slightly poorer resolution than the DFB laser with single pulses, as reported in [6]. This additional inaccuracy in FP lasers, observed at same input peak power, can be a consequence of a small drift affecting the modes of the FP laser in the μs-scale and related to the wavelength dependence of the BFS, in such a way that each FP mode generates a slightly different BFS inducing a small additional broadening factor in the measured Brillouin spectrum. The measured Brillouin linewidth is actually ~50 MHz, thus slightly reducing the BFS measurement resolution.

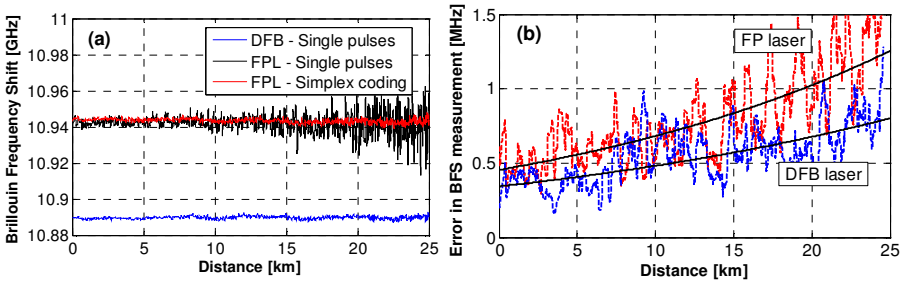

Fig. 4. (a) BFS along the sensing fiber, when using a DFB laser (single pulses) and a FP laser (Simplex coding and single pulses). (b) Error in BFS measurement vs distance for DFB laser (single pulses) and FP laser (Simplex coding).

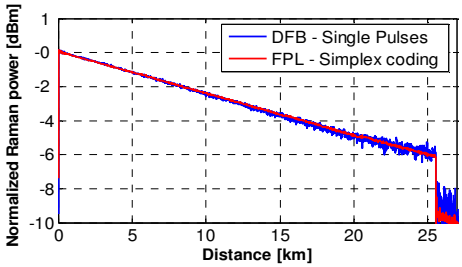

Fig. 5. Anti-Stokes Raman traces for both DFB laser (with single pulses) and FP laser (127-bit Simplex coding).

However, such additional inaccuracy observed in BFS measurement with FP laser, which degrades the resolution, is compensated by the SNR enhancement provided by Simplex coding, as shown in Fig. 4b, resulting in similar *net* BFS resolution obtained for both cases. On the other hand, Fig. 5 shows the anti-Stokes Raman traces measured for both DFB laser (with single pulses) and FP laser (with pulse coding), considering the same number of acquisitions. We can clearly observe a notably better SNR when using FP laser and coding, corresponding to ~8.7 dB resolution enhancement with respect to the use of conventional hybrid sensors (based on DFB laser and single pulses). Note that the use of coding techniques with FP laser is possible thanks to the power distribution among several longitudinal modes along the spectrum (coding cannot be applied to DFB laser due to onset of nonlinear effects [9]). Resolution for simultaneous strain and temperature measurements (obtained from Eqs. (1-2) can be calculated employing the measured standard deviation of both BFS and anti-Stokes Raman power traces. Figure 6a and Fig. 6b show a comparison of the experimental temperature and strain resolutions obtained with both DFB laser (using single pulses) and FP laser (using 127-bit Simplex coding). We can see how the temperature resolution of ~2 °C, obtained with the DFB laser at 25-km distance, is improved down to a notable value of ~0.27 °C when using the FP laser and Simplex coding, resulting in a nearly ten-fold resolution improvement (equal to almost 8.7 dB). Simultaneous strain resolution is also sensibly improved from ~60 με down to ~30 με over 25-km distance, with a ~3 dB net improvement.

#124144 - $15.00 USD Received 11 Feb 2010; revised 11 Mar 2010; accepted 12 Mar 2010; published 7 Apr 2010

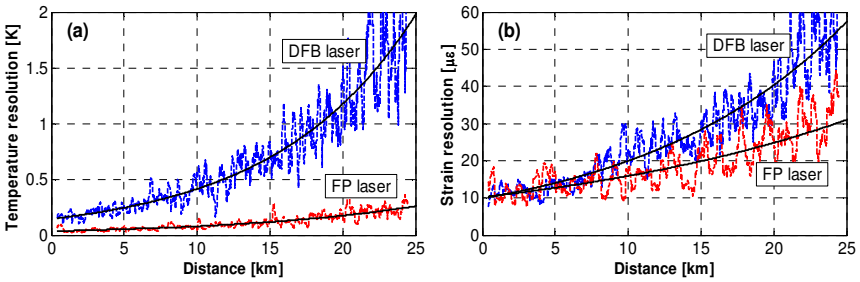

Fig. 6. (a) Temperature and (b) strain resolution vs distance, for DFB (single pulses) and FP laser (Simplex coding).

6. Conclusions

In conclusion, we have implemented a distributed hybrid Raman–Brillouin sensor combining the use of optical pulse coding techniques with high peak power FP lasers to enhance the performance of this kind of sensors, thanks to the distribution of the power into several longitudinal modes within the laser spectrum. Thus, the limitation on the maximum allowed input pulse power when using pulse coding with using narrowband sources can be overcome with FP lasers providing an effective solution to improve the performance of hybrid sensors. Experimental results indicate the achievement of a sensing resolution better than ~0.27 °C / ~30 με in temperature / strain over 25-km distance, corresponding to an improvement better than ~8.7 dB in temperature resolution and ~3 dB in strain resolution with respect to the use of standard DFB lasers. This has been achieved with a significantly simpler sensor implementation without the need of optical amplification or wavelength averaging techniques.

#124144 - $15.00 USD Received 11 Feb 2010; revised 11 Mar 2010; accepted 12 Mar 2010; published 7 Apr 2010